Pharm Res (2014) 31:2784–2795
DOI 10.1007/s11095-014-1375-6

RESEARCH PAPER

LHRH-Conjugated Micelles for Targeted Delivery of Antiandrogen to Treat Advanced Prostate Cancer

Di Wen • Deepak Chitkara • Hao Wu • Michael Danquah • Renukadevi Patil • Duane D. Miller • Ram I. Mahato

Received: 10 February 2014 / Accepted: 21 March 2014 / Published online: 2 May 2014

ABSTRACT

Purpose Our objective was to synthesize LHRH-conjugated amphiphilic copolymer for micellar delivery of CBDIV17, a novel antiandrogen for treating prostate cancer.

Methods LHRH-PEG-b-p(CB-co-LA) was synthesized by opening polymerization of carbonate (CB), lactide (LA), and HOOC-PEG-OH followed by conjugation with LHRH analogue. Bicalutamide analogue CBIDV17 loaded micelles were formulated by film hydration method, and characterized for critical micelle concentration (CMC), drug loading and *in vitro* drug release. Formulations were tested on LNCaP and C4-2 cells for cellular uptake, induction of apoptosis, viability and dowregulation of androgen receptor (AR). *In vivo* studies were performed in ectopic tumor bearing athymic nude mice after tail vein injection at a dose of 10 mg/kg. Tumor volume and body weight were measured for 25 days followed by immunohistochemistry (IHC) of tumor samples for Ki-67, caspase-3, and prostate specific antigen (PSA).

Results HOOC-PEG-b-p(CB-co-LA) and LHRH-PEG-b-p(CB-co-LA) were characterized by ^{1}HNMR and used for preparing micelles, which had a mean particle size of 75.60 ± 2.25 and 72.64 ± 1.15 nm, respectively and CBDIV17 loading of 4.6% w/w. LHRH conjugated micelles showed higher cellular uptake, cytotoxicity, and apoptosis in LNCaP and C4-2 cells compared to non-targeted micelles. CBDIV17 loaded LHRH micelles more efficiently inhibited the proliferation and induced apoptosis of tumor cells according to Ki-67, caspase-3, and PSA expression. There was significant inhibition of tumor growth with the treatment of CBDIV17 loaded LHRH-conjugated micelles.

Conclusion These results demonstrated that LHRH-b-PEG-p (CB-co-LA) micelles have the potential for targeted delivery of CBDIV17 to treat advanced prostate cancer.

KEY WORDS antiandrogen · bicalutamide · LHRH · micelles · prostate cancer

INTRODUCTION

Androgen ablation or blockade of androgen receptor (AR) is the cornerstone of treating early stage prostate cancer. Among various antiandrogens for chemotherapy, bicalutamide has long half-life and tolerable side effects, leading to its wide clinical application for treating early stage prostate cancer (1). However, prolonged treatment with bicalutamide leads to AR proliferation and mutation, which converts bicalutamide from an AR antagonist into an AR agonist. To overcome this issue, we previously synthesized bicalutamide analog CBDIV17, which was more potent than bicalutamide in inhibiting the proliferation of prostate cancer cells and suppressing tumor growth *in vivo* (2). Despite its high efficacy, poor aqueous solubility of CBDIV17 (less than 50 mg/L) results in low and variable drug absorption.

Polymeric micelles are nanosized and have spherical structures with a hydrophobic core, which is able to improve the solubility and stability of hydrophobic anticancer drugs. To enhance the solubility of CBDIV17, we synthesized polyethylene glycol-b-poly (carbonate-co-lactide) (PEG-b-p(CB-co-LA)) copolymer (2–5) to prepare micelles, which successfully encapsulated bicalutamide, embelin, and some other drugs. In our previous results (2), CBDIV17 loaded micelles showed high antitumor efficacy and successfully suppressed tumor growth *in vivo*. However, intratumoral injection of these micelles limited its clinical application to prostate cancer.

D. Wen • D. Chitkara • R. I. Mahato
College of Pharmacy, University of Nebraska Medical Center, Omaha Nebraska 68198, USA

H. Wu • M. Danquah • R. Patil • D. D. Miller
Department of Pharmaceutical Sciences, University of Tennessee Health Science Center, Memphis, Tennessee 38163, USA

R. I. Mahato (✉)
Department of Pharmaceutical Sciences, University of Nebraska Medical Center, 986025 Nebraska Medical Center, Omaha Nebraska 68198-6025, USA
e-mail: ram.mahato@unmc.edu
URL: http://www.unmc.edu/pharmacy/mahato

Traditional chemotherapy usually employs high dose of anti-cancer drugs, which usually cause severe toxicity to healthy organs. Passive targeting tumors *in vivo* mainly utilized enhanced permeability and retention (EPR) effect (6,7) causing preferential accumulation of macromolecules at the tumor site. However, EPR effect is only efficient for targeting solid tumors and is not used for spreading tumors and metastases (8). Active targeting can be used to make micelles site-specific by coupling a target moiety for receptors overexpressed on cancer cells. Furthermore, targeting cancer cells can diminish the cytotoxicity towards other tissues and the drugs loaded micelles accumulate selectively to tumor site (9,10). For targeted delivery of anti-cancer drugs, several receptors, which are overexpressed by cancer cells, are selected as targets for polymer binding, such as prostate specific membrane antigen (PSMA) (11), epidermal growth factor receptor (EGFR) (12), and luteinizing-hormone-releasing hormone (LHRH) receptor (13).

LHRH is a 10 amino acid peptide hormone secreted by hypothalamus and regulates gametogenesis (14). Overexpressed LHRH receptors are detected in prostate (86%), ovarian (80%), and breast (50%) cancers and have low expression in healthy organs (7,15–17). In recent years, LHRH and its analogs have been employed in the clinical trial in the management of prostate cancer. We expect active targeting by LHRH to be safe and efficient after systemic administration. Due to the short half-life of natural LHRH, synthetic LHRH analogue with improved bioactivity has been widely used for targeting LHRH-R (18,19). Therefore, we conjugated LHRH analog to our previously synthesized HOOC-PEG-b-p(CB-co-LA) copolymer and hypothesize that LHRH conjugated micelles would improve the efficacy of antitumor drug *in vitro* and *in vivo* and provide targeted drug delivery to suppress tumor growth. In this study, HOOC-PEG-b-p(CB-co-LA) and LHRH-PEG-b-p(CB-co-LA) were synthesized, characterized, and used for preparing micelles for targeted delivery of CBDIV17. We evaluated the drug therapeutic efficacy of LHRH-conjugated micelles carrying CBDIV17 in an ectopic athymic mouse model of prostate cancer.

MATERIALS AND METHODS

Materials

2, 2-Bis(hydroxymethyl) propionic acid and benzyl bromide were purchased from Sigma Aldrich (St. Louis, MO). Hydroxyl poly(ethylene glycol) carboxyl (HOOC-PEG-OH, M_n = 5000) was purchased from Jenkem Technology (Allen, TX). SYBR Green, real-time RT-PCR master mix, and reverse transcription reagents were purchased from Roche (Indianapolis, IN). LHRH analog peptide, PYR-His-Trp-Ser-Tyr-^{D}Lys-Leu-Arg-Pro-Gly-$CONH_2$, was purchased from Hanhong Group (Shanghai, China). CBDIV17 was synthesized as reported earlier (2). All other chemicals were of analytical grade and used as received.

Synthesis of LHRH-PEG-b-p(CB-co-LA)

5-Methyl-5-benzyloxycarbonyl-1, 3-dioxane-2-one (MBC) and HOOC-PEG-b-p(CB-co-LA) were synthesized as described earlier (20). Briefly, 2, 2-bis(hydroxymethyl)propionic acid (26.8 g, 0.2 mol) and potassium hydroxide (12.72 g, 0.2 mol) were dissolved in 150 mL of dimethylformamide (DMF) and allowed to heat at 100°C for 1 h. Benzyl bromide (41.5 g, 0.243 mol) was then added dropwise and continuously stirred at 100°C for 15 h. DMF was evaporated under vacuum and the crude product was dissolved in ethyl acetate (150 mL), hexanes (150 mL), and water (100 mL). The organic layer was separated, washed with water, and dried with Na_2SO_4. The final solution was evaporated to obtain benzyl 2, 2-bis(methylol)propionate (23.8 g, 56.64%), which was subsequently recrystallized using toluene.

To synthesize 5-methyl-5-benzyloxycarbonyl-1,3-dioxane-2-one (MBC) (base monomer), benzyl 2, 2-bis (methylol)propionate (22.4 g, 0.1 mol) dissolved in pyridine (50 mL) and CH_2Cl_2 (200 mL), and chilled to −78°C over dry ice. A solution of triphosgene (50 mmol, 14.8 g) dissolved in CH_2Cl_2 was added dropwise to the above solution and allowed to stir for 1 h at −78°C and for additional 2 h at room temperature. The solution was quenched with saturated aqueous NH_4Cl. Organic layer was washed with 1 M HCl, saturated aqueous $NaHCO_3$ and then dried with Na_2SO_4. The pure MBC (19.7 g, 88.3%) was obtained by evaporating the organic solvent under vacuum and recrystalized using ice-cold ethyl acetate.

To synthesize HOOC-PEG-b-p(CB-co-LA) with the molecular weight of 10000, 1, 8-diazabicyclo[5.4.0]undec-7-ene (DBU) (40 μL) as a catalyst was added to the mixture of HOOC-PEG-OH (1 g), lactide (0.6 g) and base monomer (0.4 g) dissolved in 10 mL of anhydrous CH_2Cl_2 and allowed to react for 3 h under stirring at room temperature. At the end of the reaction, benzoic acid (60 mg) was added and the solvent was removed under vacuum. Crude polymer was purified by dissolving in chloroform, and precipitate in large amount of isopropanol and diethyl ether, followed by drying under vacuum for 48 h.

Purified copolymer (100 mg, 0.01 mmol) and LHRH-NH_2 (27 mg, 0.02 mmol) were dissolved in a mixture of anhydrous DMSO (3 mL) and anhydrous CH_2Cl_2 (12 mL). The mixture was allowed to stir for 30 min following which 1-Ethyl-3-(3-dimethylaminopropyl)carbodiimide · HCl (EDC · HCl) (3.0 mg, 0.0134 mM) and 4-dimethylaminopyridine (1.0 mg, 0.008 mM) were added. After 48 h, CH_2Cl_2 was removed under vacuum and the mixture was purified by dialysis

(molecular mass cutoff, 3,500 Da) using water as a solvent. Purified LHRH conjugated polymer was dried by lyophilization.

Polymers were characterized using ^{1}HNMR recorded on a Varian (500 MHz, T = 25°C) using DMSO-d_6 as a solvent. The chemical shifts were calibrated using tetramethylsilane as an internal reference and reported as parts per million.

Critical Micelle Concentration

Fluorescence spectroscopy was used to estimate the critical micelle concentration (CMC) of HOOC-PEG-b-p(CB-co-LA) and LHRH-PEG-b-p(CB-co-LA) copolymer using pyrene as a hydrophobic fluorescent probe. Sixteen samples of HOOC-PEG-b-p(CB-co-LA) or LHRH-PEG-b-p(CB-co-LA) dissolved in water with concentrations ranging from 1.0×10^{-8} to 1 g/L were prepared and allowed to equilibrate with a constant pyrene concentration of 6.0×10^{-7} M overnight at room temperature while shaking at 200 rpm. The fluorescent spectra of pyrene were recorded at an excitation wavelength of 335 nm and emission wavelength of 373 nm (I_1) and 384 nm (I_3) using spectrofluorometer (Sunnyvale, CA). Peak height intensity ratio (I_3/I_1) was plotted against the logarithm of polymer concentration. Value of the CMC was obtained as the point of intersection of two tangents drawn to the curve at high and low concentrations, respectively.

Formulation and Characterization of Drug-loaded Micelles

CBDIV17 loaded micelles were prepared using the film hydration method as previously described with slight modifications (21). Briefly, 5 mg of CBDIV17 and 95 mg of HOOC-PEG-b-p(CB-co-LA) or LHRH-PEG-b-p(CB-co-LA) were dissolved in 5 mL chloroform. Solvent was evaporated under vacuum and resulting film was hydrated in 10 mL of phosphate buffered saline (PBS), and sonicated for 10 min using a Misonix ultrasonic liquid processor (Farmingdale, NY) with an amplitude of 60. Free drug was removed by centrifugation at 5,000 rpm for 5 min and filtration using a 0.22 μm nylon filter. Drug loaded micelles were concentrated by Amicon Ultra-15 Centrifugal Filter Unit (3,000 Da) and stored at 4°C. For further characterization, mean particle size and size distribution of drug-loaded micelles were measured by dynamic light scattering using a Malvern Zetasizer (Worcestershire, UK).

Drug Loading and Encapsulation Efficiency

To determine the drug loading and encapsulation efficiency, drug loaded micelles were dissolved in acetonitrile (ACN). Concentration of CBDIV17 was measured by reverse phase high performance liquid chromatography (RP-HPLC, Waters, Milford, MA) with a UV detector at 290 nm using a reverse phase C18 Column (250 mm × 4.6 mm, Inertsil ODS). The mobile phase was composed of 60:40 V/V of acetonitrile and water. CBDIV17 concentration was calculated according to the peak area using the following standard calibration equation: A = 703400X-59.22 (R^2 = 0.999). Drug loading content and encapsulation efficiency were determined using following equations:

$$\text{Drug loading density} = \frac{\text{weight of drug in micelles}}{\text{weight of micelles}} \times 100\% \quad (1)$$

$$\text{Drug encapsulation efficiency} = \frac{\text{weight of drug in micelles}}{\text{weight of drug originally fed}} \times 100\% \quad (2)$$

In Vitro Drug Release Study

Drug release from HOOC-PEG-b-p(CB-co-LA) and LHRH-PEG-b-p(CB-co-LA) micelles was determined after dialysis (3,500 Da cut off) against 25 mL PBS containing 0.1% Tween 80 (pH = 7.2) in a thermo-controlled shaker with a speed of 100 rpm (5). 1 mL samples were taken at specific time points (1, 3, 6, 12, 24, 48, 96, 144, 192 h) and replaced with fresh PBS containing 0.1% tween 80. Drug concentration was measured using RP-HPLC as described for drug loading. Cumulative amount of drug released was evaluated as the percentage of total drug release to the initial amount. All experiments were performed in triplicate and the data reported as the mean of three individual experiments.

Cell Culture and Maintenance

Human prostate cancer cells C4-2 and lymph node prostate adenocarcinoma (LNCaP) were purchased from American Type Culture Collection (ATCC, Manassas, VA). LNCaP and C4-2 cells were cultured in RPMI 1640 media containing 10% fetal bovine serum, 1% antibiotic-antimycotic, and 1% sodium pyruvate at 37°C in humidified environment with 5% CO_2. RWPE-1 cell line was kindly provided by Dr. Ming-Fong Lin (University of Nebraska Medical Center, Omaha, NE).

Cellular Uptake of Targeted Micelles

Cellular uptake study was performed as described by Zou (22) and Kutty (23) with minor modification. LNCaP and C4-2 cells were seeded at a density of 1×10^5 cells/well in 96 well plates. After reaching confluence, medium was replaced by

coumarin-6 loaded micelles suspensions with concentration of 0.3 mg/ml. After 2 h incubation, the micelles solution was removed and cells were washed twice with 1 × PBS. The cells were examined using inverted fluorescent microscope after DAPI staining. For quantitative study, the cells were immersed in 0.5% Triton X-100 in 0.2 N NaOH solutions and concentration of coumarin-6 was measured at excitation wavelength of 430 nm, and emission wavelength of 485 nm. The reading of wells with the cells alone represented the background intensity and was set up as a negative control. The reading of the wells with coumarin-6 loaded micelles (0.3 mg/mL) was used as a positive control. The efficiency of cellular uptake was calculated as (*I*: fluorescence intensity):

$$\text{Uptake efficiency } \% = \frac{I_{sample} - I_{negative}}{I_{positive} - I_{negative}} \times 100\%$$

Cell Viability Assay

Cells were seeded in 96-well plate at a density of 5,000 cells/well to determine cytotoxicity of free, HOOC-PEG-b-p(CB-CO-LA) or LHRH-PEG-b-p(CB-CO-LA) micelles loaded with CBDIV17 at the concentration of 10, 25, 50 μmol/L for 48 h. The cellular toxicity of the two polymers was also determined in these two cell lines. At the end of the treatment, the original medium was replaced by fresh medium with 0.5 mg/mL MTT (3-(4,5-dimethylthiazol-2-yl)-2,5-diphenyltetrazolium bromide) and incubated for another two hours. The supernatant was removed carefully and MTT crystals were dissolved in 200 μl DMSO and analyzed at a wavelength of 560 nm. Cell viability was calculated as a percentage of control using the following formula:

$$\text{Cell viability } (\%) = \frac{absorbance\ \ of\ \ test\ \ sample}{absorbance\ \ of\ \ control} \times 100\%$$

Real-Time RT-PCR

Expression of LHRH receptor was determined by quantitative real-time RT-PCR. Briefly, LNCaP and C4-2 cells were seeded in 24-well plate at the density of 5×10^5cells/well overnight. Total mRNA was isolated from cultured cells using RNeasy mini isolation kit (Qiagen, Valencia, CA) and the concentration was determined by Nanodrop 2000 (Thermo Scientific, Wilmington, DE). 170 ng of total mRNA was converted to cDNA using TaqMan Reverse Transcription Reagents (Life Technologies, Grand Island, NY). cDNA was used as a template and analyzed by SYBR Green universal PCR master mix (Life Technologies, Grand Island, NY) on Roche Real-time PCR instrument. S19 was used as an internal control. All samples were run in triplicate. The primer sequences were as follows: human LHRH receptor (Type 1) (forward): 5′-GACCTTGTCTGGAAAGATCC-3′, (reverse) 5′-CAGGCTGATCACCACCATCA-3′; human S19 (forward): 5′- GGAGCTCTATCCTCTCTCTATT-3′, (reverse): 5′-CCCAGCATGGTTTGTTCTAATG-3′.

Western Blot Analysis

C4-2 (2×10^6/well) cells seeded in 6-well plate were treated with CBDIV17 loaded LHRH-PEG-b-p(CB-co-LA) with the drug concentration of 25 μmol/L for 48 h. Subsequently, cells were lysed with RIPA buffer (Sigma-Aldrich, St. Louis, MO) and protein concentration was measured with micro BCA protein assay kit (Thermo Scientific, Wilmington, DE). The lysate was then mixed with 6 × Laemmli Buffer (Bioworld, Dublin, OH) and boiled for 5 min. The samples were loaded to 4–15% SDS-PAGE for electrophoresis and subsequently transferred to immobilon polyvinylidene fluoride (PVDF) membrane. Membranes were blocked with 5% bovine serum albumin (BSA) in tris buffered saline at room temperature for 1 h and further incubated with primary antibody at 4°C overnight, followed by incubation with secondary antibody conjugated with infrared dyes (IRDye) at room temperature for 1 h. After washing with tris buffered saline and tween 20 for 3 times, the signal of target protein was detected using Li-COR Odyssey infrared imaging system (Li-COR, Lincoln, NE).

Caspase 3 Activity

Caspase 3 activity was analyzed with Caspase-Glo 3 assay kit as per manufacturer's protocol. To a single cell suspension generated by 0.25% Trypsin-EDTA digestion, 100 μL of Caspase-Glo was added with the concentration of 10^4 cells/well in 96 well plate and incubated at room temperature for 1 h. The solution was then transferred to culture tubes to determine luminescence by a luminometer (Berthold, Bad Wildbad, Germany).

In Vivo Efficacy of Drug Loaded LHRH Conjugated Micelles in Ectopic Tumor Bearing Mice

All experiments were performed following the NIH animal use guidelines and the protocol was approved by the Animal Care and Use Committee (ACUC) at the University of Nebraska Medical Center. Ectopic flank tumors were induced in 6 weeks old male athymic nude mice (Jackson Laboratory, Bar Harbor, ME) by subcutaneous injection of 2 million C4-2 cells suspended in 1:1 serum free media and Matrigel. The mice were randomized into the following three groups when the tumor size reached to 150 mm^3: i) untreated control, ii) CBDIV17 loaded non-conjugated micelles, iii) CBDIV17

loaded LHRH conjugated micelles. Formulations were injected intravenously *via* tail vein at the concentration of 10 mg/kg at 3 day intervals for 25 days. Animal body weight and tumor volume were monitored three times a week. Tumors were measured with a caliper prior to each injection, and their volumes calculated using the formula as follows:

$$\text{Volumes} = \left(\text{width}^2 \times \text{length}\right)/2 \quad (3)$$

To determine apoptosis and proliferation of tumor cells, tumors from mice were excised and fixed in 10% buffered formalin, followed by routinely proceeding to paraffin. For embedding histology, 5 μm thick sections were stained with Hematoxylin & Eosin for detection of tumor architecture. Cell proliferation and apoptosis were determined using an antibody against Ki-67 and caspase-3, respectively. The prostate cancer treatment was evaluated by PSA level.

Statistical Analysis

Statistical significance of difference between two groups was determined by unpaired *t* test.

RESULTS

Synthesis and Characterization of HOOC-PEG-b-p (CB-co-LA) and LHRH-PEG-b-p(CB-co-LA)

HOOC-PEG-b-p(CB-co-LA) copolymer was synthesized by ring opening polymerization of L-lactide and 5-methyl-5-benzyloxycarbonyl-1,3-dioxane-2-one using HOOC-PEG as the macroinitiator and DBU as a catalyst. The peak (Fig. 1a) at δ: 10.64 ppm demonstrated the carboxyl group and the multiplet peak at δ: 4–4.5 ppm confirms the successful ring opening polymerization. The following NMR peaks of copolymers were observed of the copolymers at δ: 1.25 (CH_3 in CB unit, s, 3H); δ: 1.60 (CH_3 in LA unit, s, 3H); δ: 3.51 (CH_2 in PEG, m, 4H); δ: 4.15–4.35 (CH_2 in CB main chain, m, 4H); δ: 5.10–5.16 (CH in LA unit q, 1H and CH_2 in CB side group, s, 2H); δ 7.36 (phenyl, m, 5H).

LHRH-PEG-b-p(CB-co-LA) was synthesized by conjugating NH_2 group of DLys in LHRH peptide to COOH group of HOOC-PEG-b-P(CB-co-LA). Conjugation was confirmed by ^{1}HNMR. The peak (Fig. 1c) at δ: 10.64 disappeared and new peaks were observed at δ: 6.80, δ: 6.94, δ: 7.18, δ: 7.82, δ: 8.18, δ: 8.31, δ: 8.64, δ: 8.85, and δ: 9.63 (Fig. 1f), which demonstrated the successful conjugation of LHRH peptide.

Preparation and Characterization of HOOC-PEG-b-p (CB-co-LA) and LHRH-PEG-b-p(CB-co-LA) Copolymer Micelles

We used film sonication method to formulate micelles of HOOC-PEG-b-p(CB-co-LA) and LHRH-PEG-b-p(CB-co-LA) copolymers. Mean particle size of blank and drug loaded micelles was in the range of 72.64-98.91 nm as determined by dynamic light scattering (Table I). Our result showed that the particle size was not influenced by LHRH conjugation. Micelles were further characterized by critical micelle concentration (CMC). Similar CMC values of HOOC-PEG-b-p (CB-co-LA) and LHRH-PEG-b-p(CB-co-LA) suggest that the conjugation of LHRH does not influence the self-assembly of the polymer (Fig. 2a).

In vitro Drug Loading and Drug Release from Micelles

The amount of CBDIV17 loaded into micelles was calculated using Eq. (1) based on 5% theoretical drug loading. According to our result (Table I), CBDIV17 loading were not influenced by LHRH conjugation. CBDIV17 loading was 4.59±0.01%. There was 50% of CBDIV17 released from both micelles after 24 h. LHRH conjugation did not affect the *in vitro* release of CBDIV17 (Fig. 2b).

In Vitro Cellular Uptake

To demonstrate the effect of LHRH conjugation on cellular uptake, we first determined LHRH receptor expression on LNCaP and C4-2 cancer cells and found to be overexpressed by at least two folds as determined by real time RT-PCR (Fig. 3a), while LHRH receptor was poorly expressed on RWPE-1 cells. We then determined the cellular uptake of coumarin-6 loaded micelles. Figure 3b and c show fluorescent microscope image of LNCaP and C4-2 cells after 2 h incubation with coumarin-6 loaded non-conjugated or LHRH conjugated micelles. The nucleus stained by DAPI was circumvented by green fluorescence of coumarin-6, suggesting that the micelles were internalized in the cytoplasm. Both cell lines incubated with coumarin-6 loaded LHRH-PEG-b-p (CB-co-LA) micelles exhibited brighter fluorescence. Figure 3d and e shows fluorescent intensity reading of the two micelles in LNCaP and C4-2 cell lines. The uptake efficiency of non-conjugated micelles was 22.7% for LNCaP and 28.3% for C4-2. The uptake efficiency of LHRH-PEG-b-p(CB-co-LA) micelles was 33.1% for LNCaP and 35.3% for C4-2. There was no significant difference in the fluorescent intensity between HOOC-PEG-b-p(CB-co-LA) and LHRH-PEG-b-p(CB-co-LA) (data not shown). It can be seen that the uptake of micelles in both cell lines, which has overexpressed LHRH receptor, significantly increased with LHRH conjugation. However, LHRH conjugation did not influence cellular

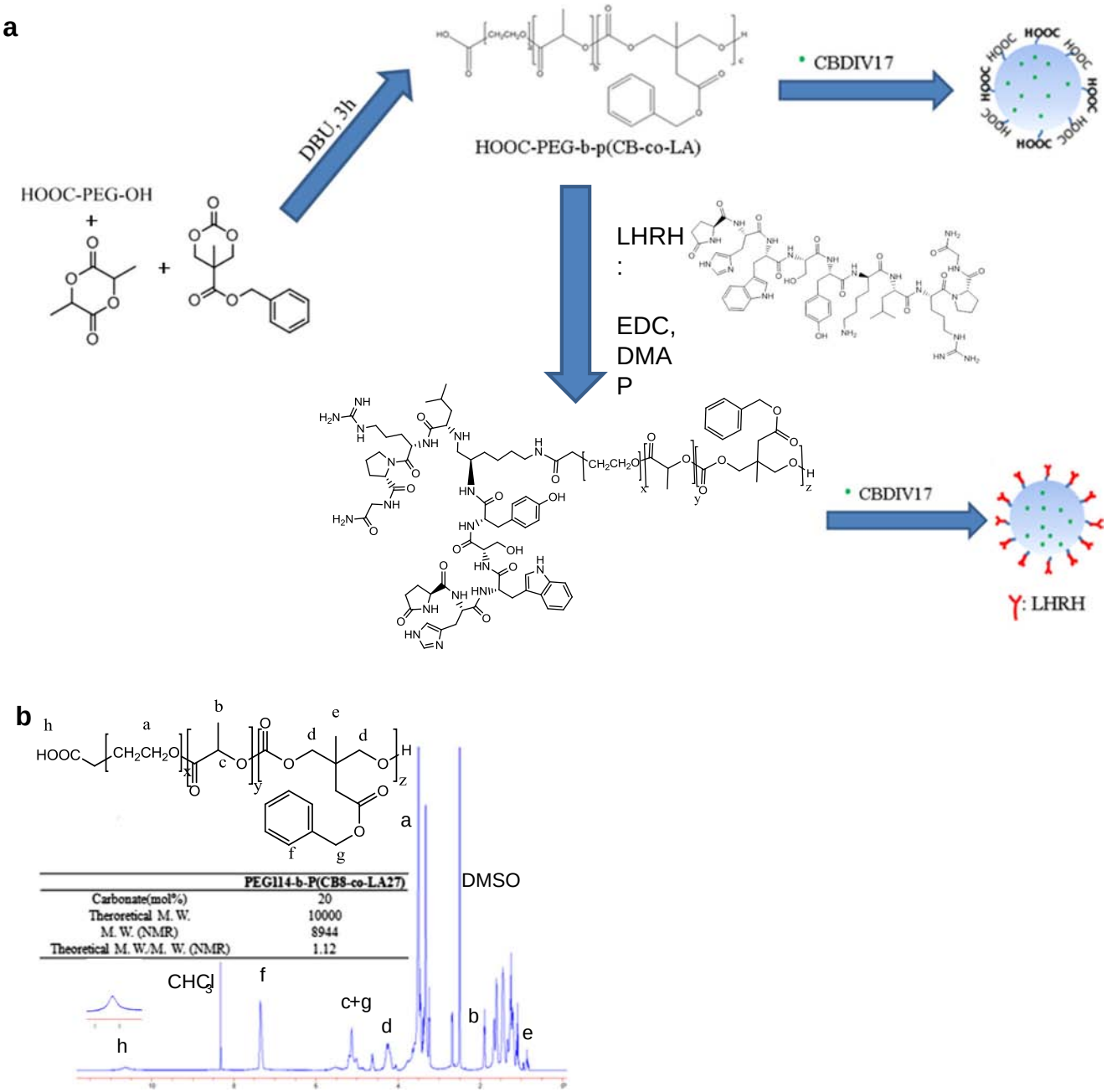

Fig. 1 Synthesis and characterization of LHRH-PEG-b-p(CB-co-LA) copolymer. (**a**) Outline of synthesis and formulation, (**b**) NMR of HOOC-PEG-b-p(CB-co-LA), (**c**) NMR of LHRH peptide and (**d**) NMR of LHRH-PEG-b-p(CB-co-LA), (**e**) Structure and NMR of LHRH peptide (ppm 6–9), (**f**) NMR of LHRH-PEG-b-p (CB-co-LA) (ppm 6–9).

uptake of micelles for RWPE-1 cells, which does not have detectable LHRH receptor, according to both fluorescent image and reading (Data not shown).

Effect of CBDIV17 Loaded LHRH-PEG-b-p(CB-co-LA) and HOOC-PEG-b-p(CB-co-LA) on LNCaP and C4-2 Growth

We determined the anticancer activity of CBDIV17 loaded micelles in LNCaP and C4-2 cells. As shown in Fig. 4a and b, CBDIV17 exhibited dose dependent anti-cancer activity in both the cell lines. Drug loaded micelles were more cytotoxic than free drug. IC50 of free CBDIV17, CBDIV17 loaded HOOC-PEG-b-p(CB-co-LA), and CBDIV17 loaded LHRH-PEG-b-p(CB-co-LA) was 25.2, 21.9, and 12.8 μM respectively in LNCaP cells. In C4-2 cells, it was 37.1, 30.9, and 19.8 μM respectively for free CBDIV17, CBDIV17 loaded HOOC-PEG-b-p(CB-co-LA), and CBDIV17 loaded LHRH-PEG-b-p(CB-co-LA) micelles. Additionally, there was a dramatic increase in the inhibition of prostate cancer cell growth

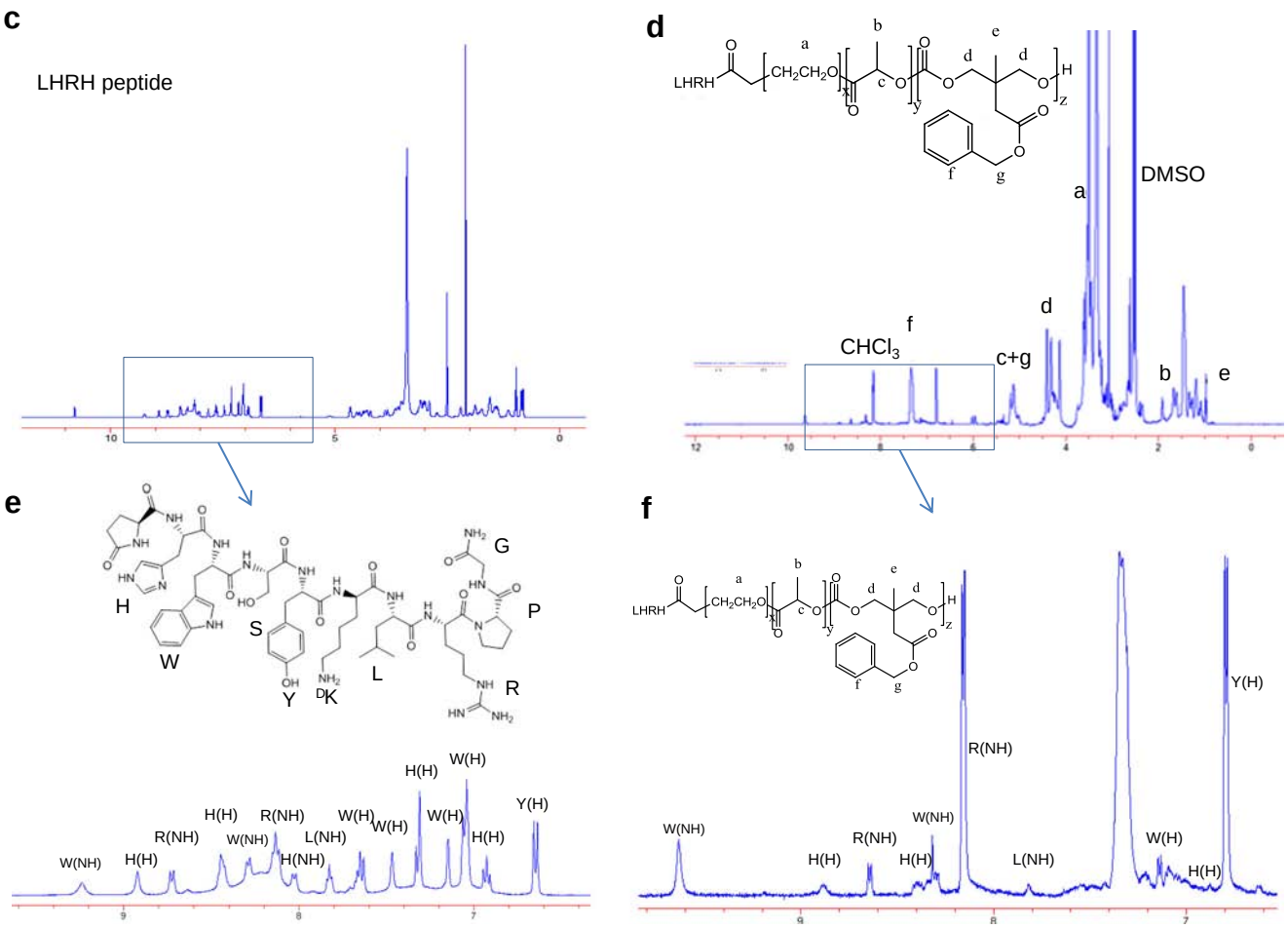

Fig. 1 (continued)

for drug loaded LHRH-PEG-b-p(CB-co-LA) micelles compared to drug loaded HOOC-PEG-b-p(CB-co-LA) micelles, suggesting LHRH conjugated micelles increased cellular uptake of CBDIV17 compared to non-conjugated micelles.

Caspase 3 and AR Activity

We next examined the influence of CBDIV loaded micelles on Caspase 3. Drug loaded micelles, especially LHRH conjugated micelles, induced more cell apoptosis than free drug according to Caspase 3 activity (Fig. 4c).

Furthermore, we determined the effect of drug loaded micelles on the transcriptional activity of AR by measuring protein expression of AR and prostate specific antigen (PSA) after treating LNCaP and C4-2 cells with 25 μmol/L LHRH-PEG-b-p(CB-co-LA) for 48 h. As shown in Fig. 4d, PSA protein expression was significantly downregulated with CBDIV17 loaded LHRH-PEG-b-p(CB-co-LA) micelles treated, while there was little effect on AR expression.

Table I Particle Size and CBDIV17 Loading (%) of HOOC-b-p(CB-co-LA) and LHRH-PEG-bp(CB-co-LA) Micelles

	Size (nm)	PDI	Drug loading (%)	Encapsulation Efficiency (%)
Before drug loading				
HOOC-PEG-b-p(CB-co-LA)	75.60 ± 2.25	0.242 ± 0.01	–	–
LHRH-PEG-b-p(CB-co-LA)	72.64 ± 1.15	0.195 ± 0.01	–	–
After CBDIV17 loading				
HOOC-PEG-b-p(CB-co-LA)	82.33 ± 3.93	0.237 ± 0.02	4.59 ± 0.01	91.80 ± 0.20
LHRH-PEG-b-p(CB-co-LA)	84.59 ± 3.29	0.197 ± 0.02	4.54 ± 0.17	90.80 ± 3.40

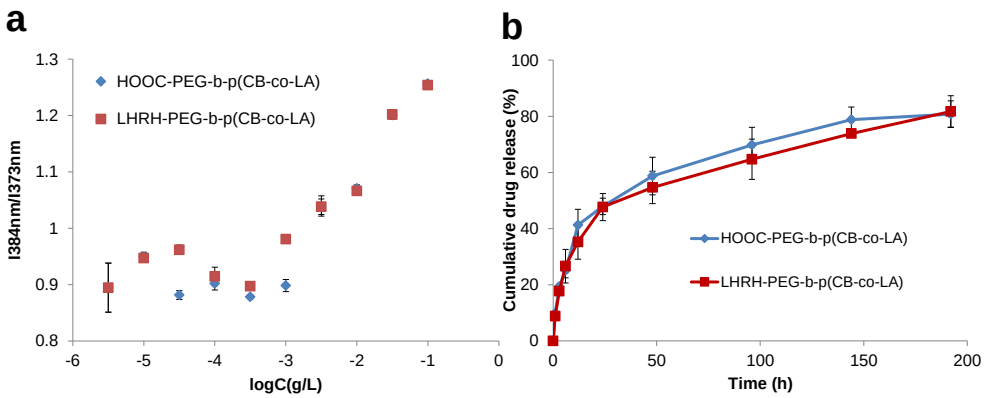

Fig. 2 Characterization of HOOC-PEG-b-p(CB-co-LA) and LHRH-PEG-b-p(CB-co-LA). (**a**) Plots of intensity ratio I_1(373 nm)/I_3(384 nm) from pyrene fluorescence emission spectra *versus* log concentration (g/L) of HOOC-PEG-b-p(CB-co-LA) and LHRH-PEG-b-p(CB-co-LA); (**b**) CBDIV17 release from HOOC-PEG-b-p(CB-co-LA) and LHRH-PEG-b-p(CB-co-LA) micelles. Release experiments were performed in triplicates. Data presented as the mean ± S.D. ($n = 3$).

In Vivo Efficacy of CBDIV17 Loaded Micelles

Since LHRH-PEG-b-p(CB-co-LA) significantly enhanced the effect of CBDIV17 *in vitro*, we further determined the effect of CBDIV17 loaded micelles in C4-2 ectopic tumor bearing athymic mice. CBDIV17 were formulated to HOOC-PEG-b-p(CB-co-LA) and LHRH-PEG-b-p(CB-co-LA) with the concentration of 2 mg/mL. The formulation was injected intravenously 4 times at the dose of 10 mg/kg at 3 day intervals. Changes in the relative tumor volume and body weight are shown in Fig. 5. Tumor growth was significantly inhibited by both CBDIV17 loaded HOOC-PEG-b-p(CB-co-LA) and LHRH-PEG-b-p(CB-co-LA) micelles. CBDIV17 loaded LHRH-PEG-b-p(CB-co-LA) micelles were more

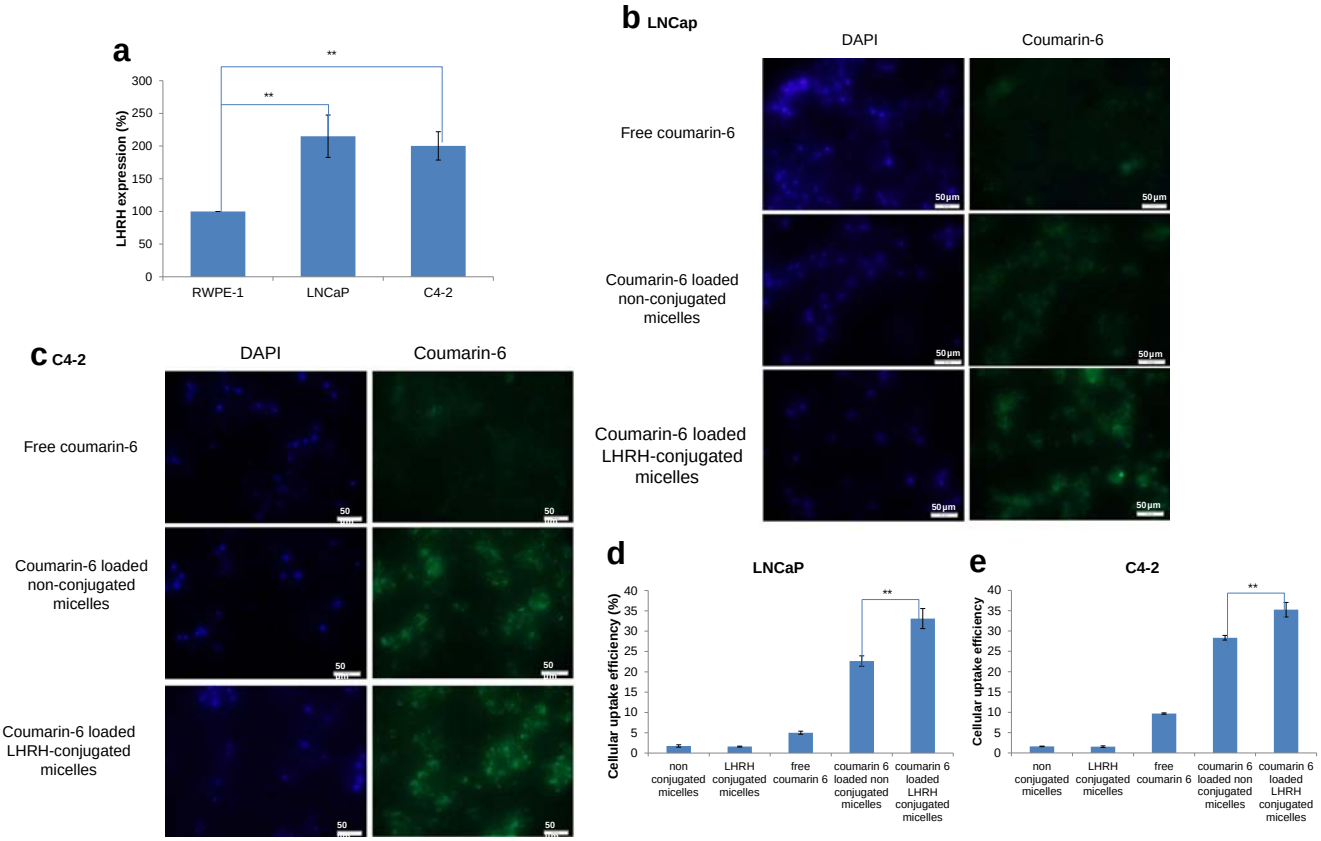

Fig. 3 Effect of LHRH conjugated micelles on the cellular uptake of antiandrogen CBDIV17. (**a**) LHRH expression by prostate cancer cells as determined by RT-PCR; (**b** and c) Fluorescent microscopy of coumarin-6 loaded LHRH-conjugated and non-conjugated micelles after incubation in LNCaP and C4-2 cells; (**d** and **e**) Cellular uptake of CBDIV17 after encapsulation into LHRH-conjugated and non-conjugated micelles. Data presented as the mean ± S.D. ($n = 3$).

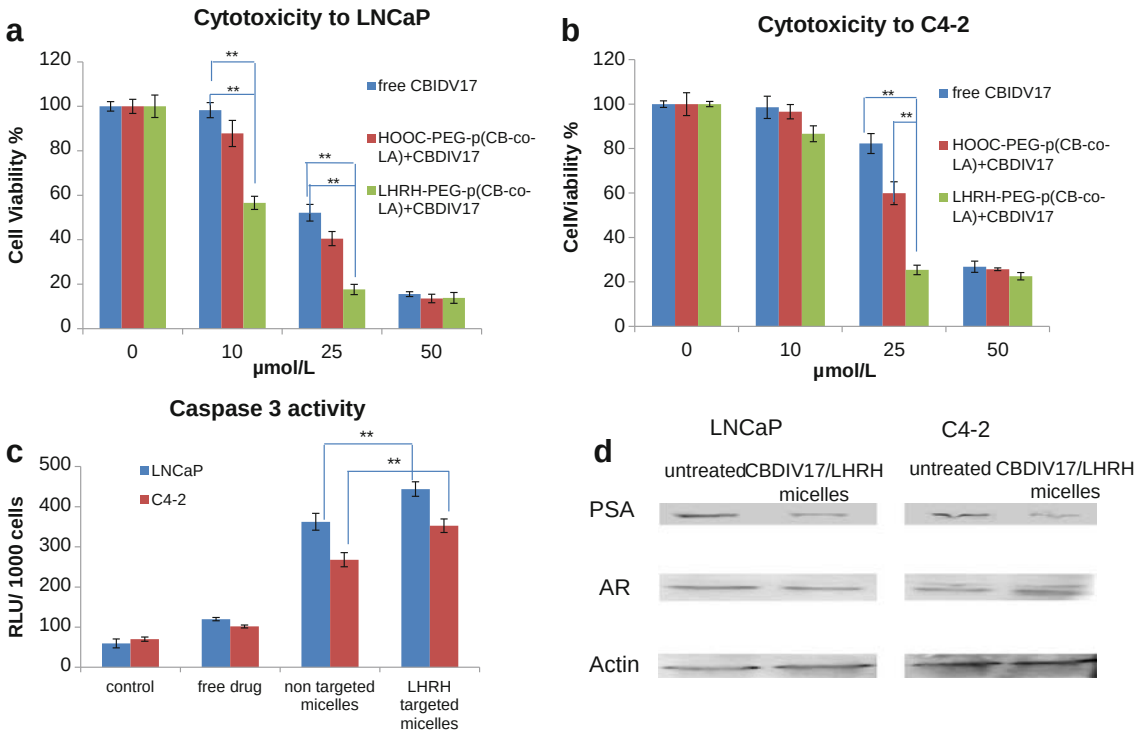

Fig. 4 Effect of HOOC-PEG-b-p(CB-co-LA) and LHRH-PEG-b-p(CB-co-LA) micellar formulation of CBDIV17 on inhibition of LNCaP and C4-2 cell proliferation. MTT assay was used for cell viability estimation. All experiments were performed in triplicates. (**a**) Cytotoxicity of CBDIV17 loaded micelles to LNCaP cells. (**b**) Cytotoxicity of CBDIV17 loaded micelles to C4-2 cells. (**c**) Caspase 3 activity after treating with 25 μmol/L CBDIV17 for 48 h. (**d**) Western blot of PSA and AR after 25 μmol/L CBDIV17 loaded micelles treated for 48 h.

effective in inhibiting tumor growth compared to CBDIV17 loaded HOOC-PEG-b-p(CB-co-LA) micelles. No significant loss in body weight was observed in the whole study, suggesting acceptable toxicity of the treatment (Fig. 5b).

On day 17, the tumors from these three groups were excised and incubated with Ki-67 and Caspase-3 antibodies to elucidate the mechanism of tumor suppression (Fig. 6). The number of cell proliferation marker Ki-67 positive cells in the control group was significantly higher compared to the mice that received CBDIV17 loaded HOOC-PEG-b-p(CB-co-LA) and LHRH-PEG-B-P(CB-CO-LA) micelles, indicating that micellar delivery of CBDIV17 efficiently suppressed tumor growth. There were only minor Ki-67 positive cells in tumor tissues from the mice injected with CBDIV17 loaded LHRH-PEG-b-p(CB-co-LA) micelles. CBDIV17 loaded LHRH-PEG-b-p(CB-co-LA) micelles were the most efficient in inducing cell apoptosis to the tumor tissues, leading to high Caspase-3 expression. Furthermore, nucleus intensity of

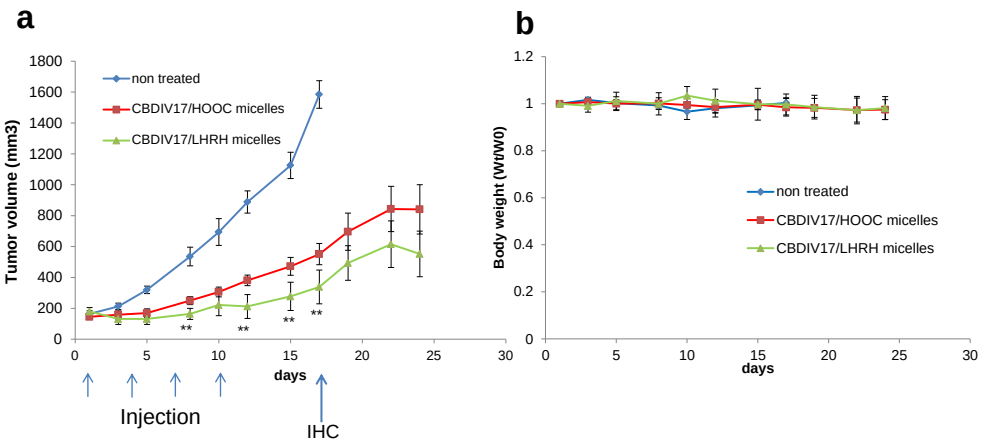

Fig. 5 Effects of CBDIV17/HOOC-PEG-b-p(CB-co-LA) and CBDIV17/LHRH-PEG-b-p(CB-co-LA) micelles on tumor growth *in vivo* (**a**) Tumor growth curve (**b**) Body weight. The number of mice use per group was 5.

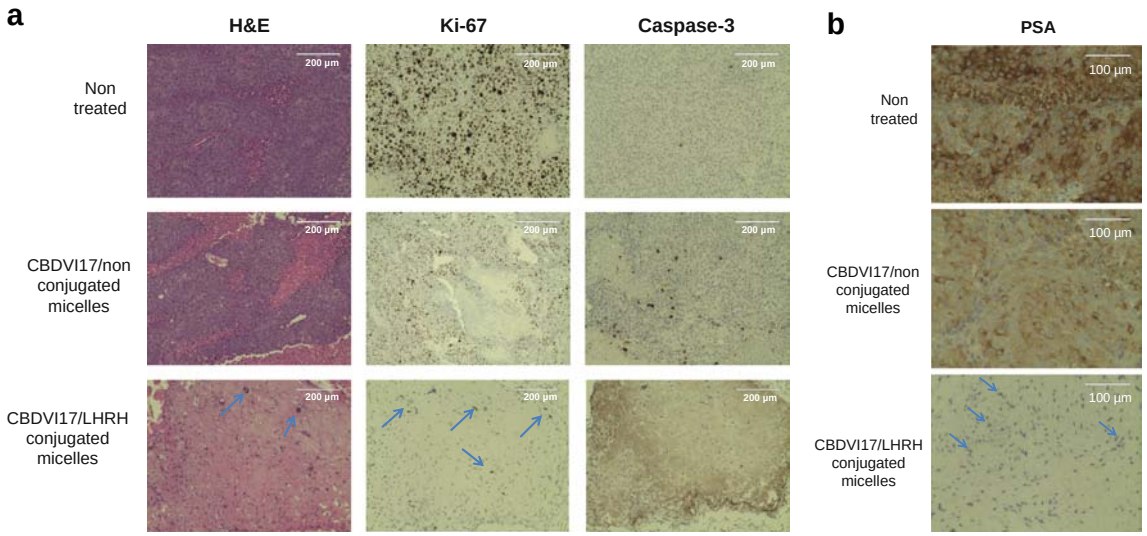

Fig. 6 Effects of CBDIV17 loaded HOOC-PEG-b-p(CB-co-LA) and LHRH-PEG-b-p(CB-co-LA) micelles on Ki-67, Caspase-3, and PSA expression in tumor.

CBDIV17/LHRH-PEG-b-p(CB-co-LA) group was obviously less other two groups, suggesting tumor growth has been successfully suppressed. Enhanced Caspase-3 expression was also observed in CBDIV17 loaded HOOC-PEG-b-p(CB-co-LA) treated tumor compared to control group, which proved antitumor efficacy of non-target delivery of CBDIV17.

DISCUSSION

Androgen inhibition is the first choice for treating early stage prostate cancer. However, AR mutation and drug resistance after prolonged treatment makes this approach less effective. Thus, more potent drugs to block androgen activity are necessary to treat advanced prostate cancer. We have previously shown that CBDIV17 was more potent than bicalutamide in inhibiting the proliferation of LNCaP and C4-2 cells (2). However, the poor solubility of CBDIV17 (less than 50 mg/L) limits its potential applications. To solve this issue, we thereby have formulated polymeric micelles, which solubilize the drugs with their hydrophobic core. Furthermore, polymeric micelles exhibit passive targeting due to the enhanced permeability and retention (EPR) effect causing preferential accumulation in tumors and inflammation sites. For targeted delivery of drug loaded micelles to the tumors, LHRH peptide was conjugated to HOOC-PEG-b-p (CB-co-LA) copolymer for targeting delivery of CBDIV17 to tumor site after systemic administration. LHRH peptide provides an effective targeting ligand to LHRH receptors overexpressed in prostate cancer cells and limited drug accumulation in normal organs, where LHRH receptors are not expressed detectably. Due to the wide application of LHRH analog, such as leuprolide, buserelin and histrelin, in the clinical trials, active targeting by LHRH analog are expected to be safe and efficient.

A modified synthetic analog of LHRH, which has free amine group to be linked with polymer without affecting its function, was used as a targeting moiety to LHRH receptors. Therefore, the choice of conjugation with –COOH or –NHS was offered (24,25). According to our NMR spectra and cytotoxicity results, the conjugation of LHRH with HOOC-PEG-b-p(CB-co-LA) was successful and there was significant difference in cytotoxicity when LHRH was conjugated to the micelles. Our results suggest that—COOH is efficient to be connected with LHRH for targeting LNCaP and C4-2 cells. LHRH conjugation did not affect the release profile of CBDIV17 (Fig. 2b). After LHRH conjugation, cellular uptake was significantly enhanced in LHRH receptor overexpressed cell lines (Fig. 3).

LHRH has been an effective systemic treatment for prostate cancer for the past 7 decades (26). Thus, we first demonstrated the non-cytotoxicity of free LHRH analog, HOOC-PEG-b-p(CB-co-LA), and LHRH-PEG-b-p(CB-co-LA) (data not shown). We observed significant cytotoxicity caused by LHRH conjugated micelles with 10 μM of CBDIV17 in LNCaP cells and 25 μM in C4-2 cells after incubating for 48 h (Fig. 4a and b). Significantly lower IC 50 demonstrated higher efficacy and cellular uptake of CBDIV17 after coating with LHRH-PEG-b-p(CB-co-LA). Blockage of androgen activity did not show high efficiency in C4-2 cells, which is androgen independent. Significantly higher Caspase 3 activity was also observed upon treatment with CBDIV17 loaded LHRH-PEG-b-p(CB-co-LA) micelles as compared to free drug and drug loaded by non-conjugated micelles, suggesting higher cell apoptosis.

PSA, which is a pivotal downstream target gene of androgen receptor (27), is always elevated in the presence of prostate

cancer and other prostate disorders. Blocking AR would reduce the transcription activity of AR, which reduces the expression of PSA. Our data (Fig. 4d) showed that AR protein expression was not influenced by CBDIV17 loaded LHRH-PEG-b-p(CB-co-LA) micelles while PSA expression was significantly inhibited. These results were similar to previously published results of bicalutamide (28,29). It means CBDIV17 does not downregulate AR expression but binds to AR and prevent AR activation, which is same as the mechanism of bicalutamide.

Following *in vitro* characterization, CBDIV17 were formulated and concentrated to HOOC-PEG-b-p(CB-co-LA) or LHRH-PEG-b-p(CB-co-LA) to evaluate tumor suppression efficacy in mice bearing C4-2 xenografts. Consistent with *in vitro* data, CBDIV17loaded LHRH-PEG-b-p(CB-co-LA) micelles was more potent in repressing prostate tumor growth compared to CBDIV17 loaded HOOC-PEG-b-p(CB-co-LA) and control groups. To further determine the mechanism of antitumor effect, we evaluated the expression of cell proliferation marker Ki-67 and apoptosis marker Caspase-3 to elucidate cell proliferation and apoptosis level in tumor tissue. Few Ki-67 positive cells and high Caspase-3 expression level demonstrated significant *in vivo* antitumor efficacy of CBDIV17 loaded LHRH-PEG-b-p(CB-co-LA). We also observed similar but less effect of CBDIV17 loaded HOOC-PEG-b-p(CB-co-LA) and tumor growth suppression after CBDIV17 loaded HOOC-PEG-b-p(CB-co-LA) treatment, which is probably caused by EPR effect.

In conclusion, we have successfully conjugated LHRH peptide to HOOC-PEG-b-p(CB-co-LA) and demonstrated that LHRH conjugation did not affect CMC, CBDIV17 loading, and drug release profile. We also revealed the mechanism of CBDIV17 as an androgen receptor antagonist. Finally, CBDIV17 loaded LHRH-PEG-b-p(CB-co-LA) showed significant potential to suppress tumor cell growth *in vitro* and *in vivo*.

ACKNOWLEDGMENTS AND DISCLOSURES

This work is supported by an Idea Award (W81XWH-10-1-0969) from the Department of Defense Prostate Cancer Research Program. We would like to thank Dr. Ming-Fong Lin of the Department of Biochemistry and Molecular Biology, University of Nebraska Medical Center for his help in analyzing IHC figures.

REFERENCES

1. Blackledge G. Casodex–mechanisms of action and opportunities for usage. Cancer. 1993;72(12 Suppl):3830–3.
2. Danquah M, Duke 3rd CB, Patil R, Miller DD, Mahato RI. Combination therapy of antiandrogen and XIAP inhibitor for treating advanced prostate cancer. Pharm Res. 2012;29(8):2079–91.
3. Chitkara D, Singh S, Kumar V, Danquah M, Behrman SW, Kumar N, *et al.* Micellar delivery of Cyclopamine and Gefitinib for treating pancreatic cancer. Mol Pharm. 2012;9:2350–7.
4. Kumar V, Mundra V, Mahato RI. Nanomedicines of Hedgehog Inhibitor and PPAR-gamma Agonist for treating liver fibrosis. Pharm Res 2013 Nov 19.
5. Mundra V, Lu Y, Danquah M, Li W, Miller DD, Mahato RI. Formulation and characterization of polyester/polycarbonate nanoparticles for delivery of a novel microtubule destabilizing agent. Pharm Res. 2012;29(11):3064–74.
6. Greish K, Fang J, Inutsuka T, Nagamitsu A, Maeda H. Macromolecular therapeutics: advantages and prospects with special emphasis on solid tumour targeting. Clin Pharmacokinet. 2003;42(13):1089–105.
7. Grundker C, Gunthert AR, Millar RP, Emons G. Expression of gonadotropin-releasing hormone II (GnRH-II) receptor in human endometrial and ovarian cancer cells and effects of GnRH-II on tumor cell proliferation. J Clin Endocrinol Metab. 2002;87(3):1427–30.
8. Chandna P, Saad M, Wang Y, Ber E, Khandare J, Vetcher AA, *et al.* Targeted proapoptotic anticancer drug delivery system. Mol Pharm. 2007;4(5):668–78.
9. Minko T. Drug targeting to the colon with lectins and neoglycoconjugates. Adv Drug Deliv Rev. 2004;56(4):491–509.
10. Minko T, Dharap SS, Pakunlu RI, Wang Y. Molecular targeting of drug delivery systems to cancer. Curr Drug Targets. 2004;5(4):389–406.
11. Chen Z, Penet MF, Nimmagadda S, Li C, Banerjee SR, Winnard Jr PT, *et al.* PSMA-targeted theranostic nanoplex for prostate cancer therapy. ACS Nano. 2012;6(9):7752–62.
12. Yip WL, Weyergang A, Berg K, Tonnesen HH, Selbo PK. Targeted delivery and enhanced cytotoxicity of cetuximab-saporin by photochemical internalization in EGFR-positive cancer cells. Mol Pharm. 2007;4(2):241–51.
13. Taratula O, Kuzmov A, Shah M, Garbuzenko OB, Minko T. Nanostructured lipid carriers as multifunctional nanomedicine platform for pulmonary co-delivery of anticancer drugs and siRNA. J Control Release. 2013;171(3):349–57.
14. Delves PJ, Lund T, Roitt IM. Antifertility vaccines. Trends Immunol. 2002;23(4):213–9.
15. Dharap SS, Qiu B, Williams GC, Sinko P, Stein S, Minko T. Molecular targeting of drug delivery systems to ovarian cancer by BH3 and LHRH peptides. J Control Release. 2003;91(1–2):61–73.
16. Dharap SS, Minko T. Targeted proapoptotic LHRH-BH3 peptide. Pharm Res. 2003;20(6):889–96.
17. Engel J, Emons G, Pinski J, Schally AV. AEZS-108: a targeted cytotoxic analog of LHRH for the treatment of cancers positive for LHRH receptors. Expert Opin Investig Drugs. 2012;21(6):891–9.
18. Pu C, Chang S, Sun J, Zhu S, Liu H, Zhu Y, *et al.* Ultrasound-mediated destruction of LHRHa-targeted and paclitaxel-loaded lipid microbubbles for the treatment of Intraperitoneal ovarian cancer xenografts. Mol Pharm. 2014;11(1):49–58.
19. Dharap SS, Wang Y, Chandna P, Khandare JJ, Qiu B, Gunaseelan S, *et al.* Tumor-specific targeting of an anticancer drug delivery system by LHRH peptide. Proc Natl Acad Sci U S A. 2005;102(36):12962–7.
20. Danquah M, Fujiwara T, Mahato RI. Lactic acid- and carbonate-based crosslinked polymeric micelles for drug delivery. J Polym Sci A Polym Chem. 2013;51(2):347–62.
21. Danquah M, Fujiwara T, Mahato RI. Self-assembling methoxypoly (ethylene glycol)-b-poly(carbonate-co-L-lactide) block copolymers for drug delivery. Biomaterials. 2010;31(8):2358–70.

22. Zou T, Gu L. TPGS emulsified zein nanoparticles enhanced oral bioavailability of daidzin: in vitro characteristics and in vivo performance. Mol Pharm. 2013;10(5):2062–70.
23. Kutty RV, Feng SS. Cetuximab conjugated vitamin E TPGS micelles for targeted delivery of docetaxel for treatment of triple negative breast cancers. Biomaterials. 2013;34(38):10160–71.
24. Taratula O, Garbuzenko OB, Kirkpatrick P, Pandya I, Savla R, Pozharov VP, *et al.* Surface-engineered targeted PPI dendrimer for efficient intracellular and intratumoral siRNA delivery. J Control Release. 2009;140(3):284–93.
25. Jiang X, Sha X, Xin H, Chen L, Gao X, Wang X, *et al.* Self-aggregated pegylated poly (trimethylene carbonate) nanoparticles decorated with c(RGDyK) peptide for targeted paclitaxel delivery to integrin-rich tumors. Biomaterials. 2011;32(35):9457–69.
26. Huggins C, Hodges CV. Studies on prostatic cancer: I. The effect of castration, of estrogen and of androgen injection on serum phosphatases in metastatic carcinoma of the prostate. 1941. J Urol. 2002;168(1):9–12.
27. Saxena P, Trerotola M, Wang T, Li J, Sayeed A, Vanoudenhove J, *et al.* PSA regulates androgen receptor expression in prostate cancer cells. Prostate. 2012;72(7):769–76.
28. Wang Y, Mikhailova M, Bose S, Pan CX, deVere White RW, Ghosh PM. Regulation of androgen receptor transcriptional activity by rapamycin in prostate cancer cell proliferation and survival. Oncogene. 2008;27(56):7106–17.
29. Colquhoun AJ, Venier NA, Vandersluis AD, Besla R, Sugar LM, Kiss A, *et al.* Metformin enhances the antiproliferative and apoptotic effect of bicalutamide in prostate cancer. Prostate Cancer Prostatic Dis. 2012;15(4):346–52.